

MULTICOLOR INFRARED OBSERVATIONS OF SN 2006aj. I. THE SUPERNOVA ASSOCIATED WITH XRF 060218

DANIEL KOCEVSKI,¹ MARYAM MODJAZ,² JOSHUA S. BLOOM,¹ RYAN FOLEY,¹ DANIEL STARR,³ CULLEN H. BLAKE,²
EMILIO E. FALCO,² NATHANIEL R. BUTLER,¹ MIKE SKRUTSKIE,⁴ AND ANDREW SZENTGYORGYI⁵

Received 2006 December 18; accepted 2007 March 9

ABSTRACT

We report simultaneous multicolor near-infrared (NIR) observations of the supernova associated with X-ray flash 060218 during the first 16 days after the high-energy event. We find that the light curve rises and peaks relatively fast compared to other Type Ic supernovae (SNe Ic), with the characteristic broad NIR peak seen in all three bands. We find that the rise profile before the peak is largely independent of NIR wavelength, each band appearing to transition into a plateau phase around day 10–13. Since the light curve is in the plateau phase when our observations end at day 16, we can only place limits on the peak absolute magnitudes, but we estimate that SN 2006aj is one of the lowest NIR luminosity X-ray flash/gamma-ray burst (XRF/GRB) associated SNe observed to date. The broad peaks observed in the JHK_s bands point to a large increase in the NIR contribution of the total flux output from days 10–16. This evolution can be seen in the broad color and spectral energy distribution diagrams constructed using $UBVRJJK_s$ monochromatic flux measurements for the first 16 days of the event. Ultimately, a 10 day rise time would make SN 2006aj an extremely fast rise SN Ic event, faster than SN 1998bw and SN 2003dh, which combined with its underluminous nature indicates a lower amount of ^{56}Ni ejected by the progenitor compared to other XRF/GRB-SNe. Furthermore, the lack of significant color change during the rise portion of the burst points to little or no spectral evolution over the first 10 days of activity in the NIR.

Subject heading: gamma rays: bursts

Online material: color figures

1. INTRODUCTION

There is now a growing body of evidence to suggest that most long-duration, soft-spectrum gamma-ray bursts (GRBs) are associated with the core collapse of massive stars. This connection had long been suggested on theoretical grounds (Colgate 1968; Woosley 1993) as well as due to the similarities between GRB and supernovae (SNe) energetics. As of early 2006, this connection had been solidified by the detection of a total of three GRBs (GRB 980425/SN 1998bw, GRB 031203/SN 2003lw, and GRB 030329/SN 2003dh) with direct spectroscopic connections to SN events (see Woosley & Bloom 2006 for a recent review). The early optical spectra of these SNe components for which high-quality spectra exist show remarkable similarities, typically deficient of hydrogen and helium lines, a property consistent with Type Ic supernovae (SN Ic). Furthermore, very broad absorption lines of O I, Ca II, and Fe II indicate high expansion velocities and a kinetic energy (E_K) going much higher than the values inferred in typical SN Ic events. Despite great interest in understanding the GRB-SN connections, only a few events have been observed well in the infrared (IR) (Lipkin et al. 2004; Cobb et al. 2006; Bloom et al. 2004). Since estimates of E_K and the amount of ^{56}Ni produced in the explosion depend on the total bolometric output,

IR observations become particularly important for our understanding of the fundamental properties of these events.

On 2006 February 18 at 03:34:30 UTC the *Swift* spacecraft detected and localized XRF 060218 (Cusumano et al. 2006a). The burst was immediately recognized as an unusual event when compared to other bursts observed by *Swift*. It was far longer than any GRB or XRF previously detected by the spacecraft, with a T_{90} duration of roughly 2000 s. It also exhibited a soft gamma-ray spectrum (Barbier et al. 2006) and an unusual afterglow that brightened for the first 10 hr after the explosion before transitioning to a more common power-law decay (Cusumano et al. 2006b; Campana et al. 2006). The first indications of an underlying SN were noted by spectra taken roughly 3 days after the event (Masetti et al. 2006) followed by reports of a rebrightening of the optical counterpart shortly thereafter (D’Avanzo et al. 2006). Like previously observed XRF/GRB-SNe the spectra of SN 2006aj showed continuum and broad-line emission with significant amounts of Fe II and Si II $\lambda 6355$ but no H or He emission. The SN 2006aj spectra best matches those of SN 2002ap and SN 1997ef at similar epochs, both broad-line SN Ic events, but neither of which have been conclusively shown to be associated with an XRF or GRB (Modjaz et al. 2006). Emission-line measurements by Mirabal et al. (2006a) gave a redshift of $z = 0.0331$, making it one of the closest XRF/GRBs ever observed, second only to GRB 980425. Such a close distance, ~ 140 Mpc, meant that XRF 060218 was similar to two other nearby XRF/GRB-SN events, GRB 980425 and GRB 031203, in that they were all significantly underluminous in the total amount of emitted gamma-ray, X-ray, and radio energies when compared to the majority of cosmological bursts (Soderberg et al. 2006). The V -band peak of SN 2006aj occurred at roughly $T = 10.0$ days (9.7 days in the rest frame) with a peak apparent magnitude of $M_V = 18.7 \pm 0.2$ mag (Modjaz et al. 2006; Sollerman et al. 2006; Mirabal et al. 2006a), making it both

¹ Astronomy Department, University of California, Berkeley, CA 94720; kocevski@berkeley.edu, jbloom@astro.berkeley.edu, froley@astro.berkeley.edu, nat@astro.berkeley.edu.

² Department of Astronomy, Harvard University, Cambridge, MA 02138; mmodjaz@cfa.harvard.edu, cblake@cfa.harvard.edu, wmwood-vasey@cfa.harvard.edu, efalco@cfa.harvard.edu.

³ Gemini Observatory, Hilo, HI 96720; dstarr1@gmail.com.

⁴ Department of Astronomy, University of Virginia, Charlottesville, VA 22903-0818; mfs4n@virginia.edu.

⁵ Harvard-Smithsonian Center for Astrophysics, Cambridge, MA 02138; saint@cfa0.cfa.harvard.edu.

the fastest evolving and least luminous of the XRF/GRB-SNe observed to date. Preburst imaging of the SN 2006aj field by the Sloan Digital Sky Survey (SDSS) provided its host galaxy magnitudes (Cool et al. 2006; Hicken et al. 2006), which given its distance reveal a low-luminosity dwarf galaxy as the host, with low metallicity (Modjaz et al. 2006; Wiersema et al. 2007), similar to the majority of other GRB host galaxies (Fruchter et al. 2006; Stanek et al. 2006; Kewley et al. 2007).

The Peters Automated Infrared Imaging Telescope (PAIRITEL) observations of XRF 060218/SN 2006aj started on February 20, well before the observed V -band and J -band peaks reported by Modjaz et al. (2006) and Cobb et al. (2006), and continued for the next 14 days. Here in Paper I we report on the light-curve properties and host-subtracted absolute magnitudes of SN 2006aj in the J , H , and K_s IR bands during these epochs. We reserve a more detailed presentation of the broadband SED evolution during this period for Paper II (M. Modjaz et al. 2007, in preparation). We present our observation and data reduction techniques and results in § 2, and discuss the implications of our observations to the further understanding of the XRF/GRB-SN phenomena in § 3.

2. DATA AND ANALYSIS

All of the IR data presented in this paper were taken with the fully automated PAIRITEL project⁶ located on Mount Hopkins in Arizona. The 1.3 m telescope contains the three Near-Infrared Camera and Multi-Object Spectrometer (NICMOS3) arrays formerly of the Two Micron All Sky Survey (2MASS) project (Skrutskie et al. 2006) to simultaneously read near-infrared (NIR) J -, H -, and K_s - (1.2, 1.6, and 2.2 μm , respectively) band images. Each image consists of a 256×256 array with a pixel scale of 2 arcsec pixel⁻¹ and an integration time of 7.8 s per image. These individual images are dithered in order to correct for bad pixels, and mosaics are created by drizzling the images, producing a Nyquist-sampled image with a pixel scale of 1 arcsec pixel⁻¹. The telescope's entire operating software has been built on the Python programming language and allows for autonomous operation, which can be monitored and controlled remotely (Bloom et al. 2006), making it excellent for the follow-up of transient events.

Observations of XRF 060218 began on the morning of February 20 and continued until the object fell below our air-mass limits some 16 days later. A total of >9000 individual images were taken in the J , H , and K_s wave bands to produce a total of 96 reduced mosaics. The individual images were dithered through a predetermined pattern for a single epoch of observations and then reduced through a custom pipeline. Bias and sky frames for each image were produced by median-combining several dithered exposures before and after the frame, whereas archival frames were used for the bad-pixel masks and flat fields. The final mosaics were produced using a drizzle technique (Fruchter & Hook 1997) for each epoch and filter with an equivalent exposure time ranging between 2 and 30 minutes. The average exposure time of each mosaic generally increased as the object moved to higher air mass in subsequent nights. Of the 96 mosaics produced through the automated reduction pipeline, three were unusable due to poor transmission on three nights, leaving ~ 31 usable mosaics per filter. An example of a stacked J, H, K_s color composite PAIRITEL mosaic can be seen in Figure 1.

A custom pipeline was used to perform photometry of the final J, H , and K_s mosaics, using aperture photometry via the SExtractor package (Bertin & Arnouts 1996) and point-spread function (PSF) photometry via the NSTAR routine in IDL to

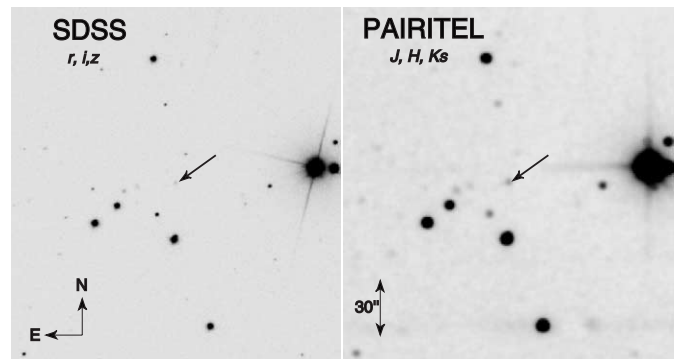


FIG. 1.—Color composite finding charts of the host galaxy (seen in SDSS preimaging; *left*) and SN 2006aj (seen in PAIRITEL; *right*). The SDSS image is made using (r, i, z)-band images (Cool et al. 2006) and the IR image using J, H, K_s from stacked mosaics obtained on 2006 March 3 UT, near in time to the peak of the optical emission of the SN. North is up, and east is to the left. [See the electronic edition of the *Journal* for a color version of this figure.]

estimate the instrumental magnitudes of every object in each mosaic. These values were then compared to the original 2MASS catalog of the same field for zero-point determination of each reduced frame. Finally, an IDL routine was employed to produce a light curve for every stellar object in the field for a final relative calibration. The resulting median Δm variations in these stellar light curves allow for additional corrections to be made to the SN light curve that account for any errors in the zero pointing of the individual mosaics.

Overall, we find that the aperture and PSF fitting routines generally yield equivalent values for J -, H -, and K_s -band mosaics. We ultimately chose to use aperture photometry with a floating aperture radius roughly equal to 1.5, 1.75, and 2.0 times the seeing (FWHM) for the J, H , and K_s bands, respectively. These factors were empirically determined to maximize the signal-to-noise ratio in each band and result in aperture radii roughly ranging from 3 to 5 pixels.

To account for the host galaxy contribution in the SN light curve, we employ a modified version of the ISIS image subtraction routine developed by Alard (2000). We revisited the XRF 060218 field 9 months after our original observations to obtain deep template imaging of the host galaxy when the SN contribution was negligible. In all, we obtained an effective exposure of roughly 5.5 hr in the J, H , and K_s bands after co-adding several nights of imaging of the host galaxy. Using this late-time template, we were able to produce residual images containing the measured flux contribution minus the host galaxy, leaving only the SN flux. In order to quantify the error involved in this subtraction process, we inserted a series of fake stars into the original mosaics and tracked the changes in their known magnitude through each subtraction. The resulting variations in the fake star light curves are then accounted for in the final host-subtracted SN light curve. We find that the host galaxy's flux contribution to the uncorrected SN light curve in most of the subtractions is roughly equal to the host magnitude found in the late-time template imaging, indicating that the host galaxy can be treated as a point source at the resolution of our images. This allows us to subtract the host contribution in catalog space in order to reduce the scatter in the final SN light curve. Our host-subtracted photometry of XRF 060218/SN 2006aj can be found in Table 1.

3. RESULTS

Figure 2 shows our host-subtracted JHK_s light curves for SN 2006aj over the course of the first 16 days since the burst plotted

⁶ See <http://www.pairitel.org>.

TABLE 1
HOST-SUBTRACTED PHOTOMETRY OF XRF 060218/SN 2006aj

Days Since GRB ^a	<i>J</i> Band ^b (mag)	<i>H</i> Band ^b (mag)	<i>K_s</i> Band ^b (mag)	Seeing (arcsec)	Air Mass (sec z)
1.99.....	18.31 ± 0.09	17.97 ± 0.21	17.72 ± 0.48	2.93	1.10
2.98.....	18.18 ± 0.09	18.04 ± 0.33	17.26 ± 0.15	2.64	1.11
4.01.....	17.85 ± 0.19	17.89 ± 0.17	17.10 ± 0.10	2.76	1.20
4.98.....	17.58 ± 0.02	17.59 ± 0.13	16.91 ± 0.20	2.77	1.22
5.98.....	17.25 ± 0.05	17.34 ± 0.13	16.63 ± 0.42	2.89	1.32
6.96.....	17.15 ± 0.07	17.15 ± 0.11	16.69 ± 0.10	2.85	1.32
7.97.....	17.12 ± 0.04	17.13 ± 0.30	16.28 ± 0.11	2.92	1.43
8.96.....	16.96 ± 0.06	16.89 ± 0.11	16.35 ± 0.16	2.95	1.29
9.98.....	17.14 ± 0.07	16.79 ± 0.04	...	2.85	1.29
12.98.....	16.88 ± 0.04	16.85 ± 0.03	16.32 ± 0.21	1.45	1.21
13.99.....	16.97 ± 0.02	16.73 ± 0.05	...	2.82	1.22
14.96.....	16.89 ± 0.03	16.83 ± 0.05	16.48 ± 0.09	2.64	1.39
16.00.....	16.93 ± 0.05	2.83	1.37

^a Observer frame.

^b Uncorrected for extinction.

in the observer frame, with the *H* and *K_s* bands shifted by 0.9 and 1.5 mag, respectively, for clarity. Each data point reflects the median average of all observations taken in a single night of observations. The error bars represent the 1 σ standard deviation about this median magnitude added in quadrature to the individual photometric measurement errors of a single mosaic. On nights in which only one mosaic was available, only the photometric error was used, which is most likely an underestimate of the true (statistical+systematic) error.

The characteristic broad peak of SN Ic events can be seen in all three bands, where the light curves flatten between day 10 and 13, with the *K_s*-band peak being more uncertain due to a gap in the available data. Cobb et al. (2006) has reported on *J*-band data peaking around day 17, just beyond our observability range, so we may miss the peak magnitude in *J* by a day. To estimate the peak magnitudes of our data set, we employ a spline fit to the light

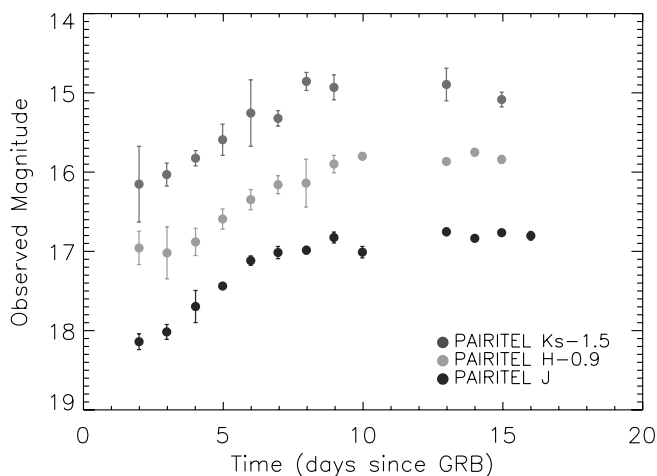


FIG. 2.—Plot of the *J*-band (black circles), *H*-band (light gray circles), and *K_s*-band (dark gray circles) aperture photometry light curve of XRF 060218/SN 2006aj after subtraction of the host contribution. The *H*- and *K_s*-band light curves have been shifted by -0.9 and -1.5 mag, respectively, for clarity. The three light curves have been corrected for Galactic and host line-of-sight extinction. The error bars represent the quadrature sum of the photometric errors associated with all the mosaics produced in a single night of observations plus the 1 σ standard deviation about their median magnitude. A flattening of the light curves in all wave bands can be seen by day 16. [See the electronic edition of the *Journal* for a color version of this figure.]

curve of each individual filter and measure apparent peak magnitudes of *J*: 16.76 ± 0.03 , *H*: 16.65 ± 0.05 , and *K_s*: 16.39 ± 0.21 . Our estimate of the *J*-band peak is consistent with the peak *J*-band measurements made by Cobb et al. (2006) of the SN and host of 16.65 ± 0.06 mag at day 17, one day after our last observation. Both the *H* and *K_s* bands are expected to peak after the *J* band, so the above values can only act as upper limits to the *HK_s* peak magnitudes. All three PAIRITEL bands appear to transition to the plateau phase at roughly the same time, with the *J* band possibly preceding the *H* and *K_s* bands. The Galactic line-of-sight extinction values for each of the bands, $A_J = 0.112$, $A_H = 0.071$, $A_{K_s} = 0.045$ (Schlegel et al. 1998), have been subtracted from the apparent peak magnitudes. Extinction from the host galaxy has been estimated by Guenther et al. (2006) through the measurements of the equivalent width (EW) of the Na I D lines along the line of sight. They find that most of the extinction is attributable to our Galaxy with a visual Galactic extinction of $A_V = 0.39 \pm 0.02$ mag and a corresponding visual host frame extinction of $A_V = 0.13 \pm 0.01$ mag. If we assume a ratio of total-to-selective extinction of $R_V = 3.1$ (Cardelli et al. 1989), we estimate NIR extinction values from the host galaxy of roughly $A_J = 0.035$, $A_H = 0.022$, $A_{K_s} = 0.015$ mag, which is considerably less than the extinction due to the line of sight through our own Galaxy. Because the well-studied hosts (Vreeswijk et al. 2004; Jakobsson et al. 2003; Savaglio & Fall 2004; Watson et al. 2006; Butler et al. 2006) of both nearby and cosmological GRBs appear to have a lower dust-to-metal ratio than the Milky Way and probably flatter extinction laws, we also consider total-to-selective extinction values of $R_V = 2.0$ (5.0), which yield roughly $A_J = 0.035$ (0.035), $A_H = 0.024$ (0.022), $A_{K_s} = 0.015$ (0.015) mag. None of these values deviate significantly from the $R_V = 3.1$ assumption, and the effects on the final light curves are within the error of our photometry. At a distance of ~ 141 Mpc ($z = 0.0335$, $H_0 = 72$ km s $^{-1}$, $\Omega_m = 0.3$, $\Omega_\Lambda = 0.7$) the peak absolute magnitude in *J* and the upper limit in *H* and *K_s*, taking into account both sets of extinction values, comes to *J*: -19.02 ± 0.03 , *H*: -19.13 ± 0.05 , and *K_s*: -19.39 ± 0.24 . In this case, these values are not *k*-corrected due to the low redshift of the event. Photometry from the deep late-time images gives the host galaxy's *JHK_s* apparent magnitudes of *J*: 18.99 ± 0.16 , *H*: 18.52 ± 0.22 , and *K_s*: 18.73 ± 0.34 , uncorrected for Galactic extinction. This represents 33.6%, 36.7%, and 27.8% of the *J*, *H*, and *K_s* flux contribution to the SN light curve at early times, respectively.

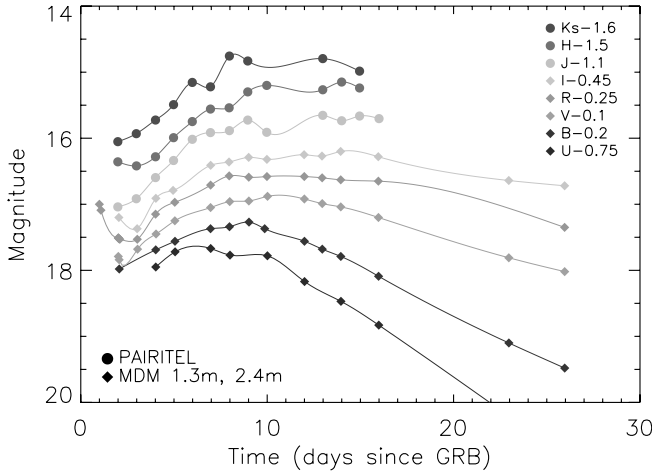


FIG. 3.—Our NIR PAIRITEL light curves plotted along with *UBVRI* data taken from Mirabal et al. (2006b). A steady progression of wider light curves at longer wavelengths is clearly seen. [See the electronic edition of the Journal for a color version of this figure.]

It should be noted that fits to the early X-ray data (Butler 2007) collected by the *Swift* spacecraft show evidence for excess X-ray absorption beyond that due to our Galaxy alone $N_{\text{H,Galactic}} = 1.11 \times 10^{21} \text{ cm}^{-2}$ (Dickey & Lockman 1990); $N_{\text{H}} = 2.9 \pm 0.5 \times 10^{21} \text{ cm}^{-2}$, at $z = 0.033$. Galactic extinction (Cardelli et al. 1989) and the Galactic A_V - N_{H} relation (Predehl & Schmitt 1995) would then imply the following absorption magnitudes in addition to the absorption by the Galaxy: $A_J = 0.51 \pm 0.07$, $A_H = 0.33 \pm 0.04$, $A_{K_s} = 0.21 \pm 0.03$. These extinction values disagree with the values calculated through the use of the EW of the Na I D by Guenther et al. (2006) and highlights the uncertainty in applying the host galaxy extinction correction. Thus, the X-ray inferred results are not subtracted from our photometry stated above but should be considered as upper limits to the possible extinction from the host galaxy. We briefly discuss possible explanations to these extinction disagreements in § 3.

We compare the observer frame NIR light curve to the light-curve behavior at optical wavelengths in Figure 3. Here we plot our *JHK_s* photometry along with *UBVRI* measurements made by Mirabal et al. (2006b) for the first 26 days of the event using the 1.3 and 2.4 m MDM telescopes. Each of the individual light curves is connected with a cubic spline for clarity. The final Mirabal et al. (2006b) photometry that we adopt for our light-curve comparison is host-subtracted and extinction-corrected assuming apparent host magnitudes of $U = 20.10$, $B = 20.41$, $V = 20.09$, $R = 19.91$, and $I = 19.54$; and Galactic extinction of $A_U = 0.77$, $A_B = 0.61$, $A_V = 0.47$, $A_R = 0.38$, and $A_I = 0.28$. The previously observed trend of broader light curves at longer wavelengths can be seen when comparing the turnover time in the shorter wavelengths compared to our *JHK_s* measurements. The detailed modeling of the light-curve behavior and the time-dependent radiative transfer calculations required for a full understanding of this trend have been accomplished for the case of SNe Ia (Kasen 2006), but have yet to be done for SNe Ib/c and are beyond the scope of this paper. This increase in the NIR flux contribution at late times can be seen nicely in the color diagram shown in Figure 4. Here we display our host-subtracted and extinction-corrected *J*-band photometry minus the *UBVRI* data from Mirabal et al. (2006b) and our *HK_s* PAIRITEL measurements. The gradual steepening of the color differences is a function of $\Delta\lambda_{\text{eff}}$ between the two filters and quantifies the relative difference between the light-curve decay rates at shorter wave-

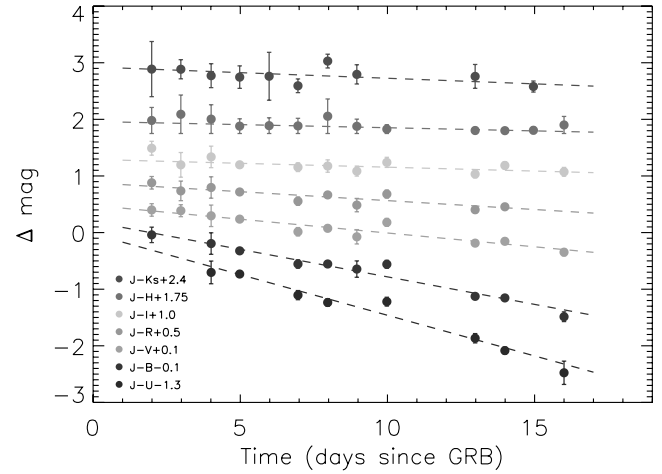


FIG. 4.—Color diagram showing the subtraction of the PAIRITEL *J*-band and *H*- and *K_s*-band data as well as the Mirabal et al. (2006b) *UBVRI* photometry. The slope of the color differences becomes steeper with increasing $\Delta\lambda_{\text{eff}}$, showing a large increase in the NIR contribution to the total bolometric flux output of the SN at later times. [See the electronic edition of the Journal for a color version of this figure.]

lengths with respect to the NIR. When fit with a linear function such that $\Delta m = \Delta m_0 - st$, the individual color difference slopes s in Figure 4 are as follows: $J-K_s$: -0.020 ± 0.012 , $J-H$: -0.011 ± 0.008 , $J-I$: -0.014 ± 0.006 , $J-R$: -0.032 ± 0.005 , $J-V$: -0.048 ± 0.005 , $J-B$: -0.097 ± 0.0046 , and $J-U$: $-0.143 \pm 0.007 \text{ mag day}^{-1}$.

The color evolution properties can also be seen in the spectral energy distribution (SED) shown in Figure 5 constructed using this same broadband *UBVRIJHK_s* photometry. We converted the *UBVRIJHK_s* photometry to monochromatic flux values using Johnson-Morgan $f_{\nu,\text{eff}}$ flux zero points from Fukugita et al. (1995) for the Mirabal et al. (2006b) data set and the 2MASS $f_{\nu,\text{eff}}$ flux zero points given in Cohen et al. (2003) for our PAIRITEL data. The figure shows several SED curves ranging from roughly 1.5 to 12 days after the *Swift* trigger as measured in the observer frame of the host galaxy; the individual SEDs are connected with

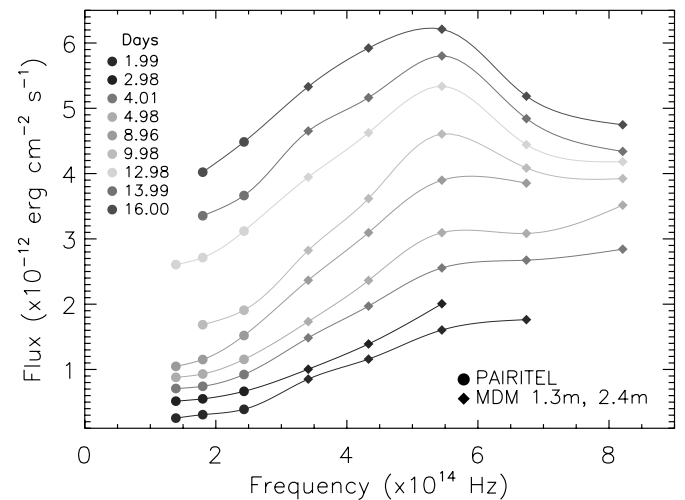


FIG. 5.—Broad SED diagram produced by converting the *JHK_s*-band data and the Mirabal et al. (2006b) *UBVRI* photometry into monochromatic flux values and plotted vs. the effective frequency of that bandpass, corrected for the redshift of the host galaxy. The NIR contribution to the total energy represented by the SED can be seen to increase at later times. [See the electronic edition of the Journal for a color version of this figure.]

TABLE 2
XRF 060218/SN 2006aj PROPERTIES

Property	<i>J</i> Band ^a (mag)	<i>H</i> Band ^a (mag)	<i>K_s</i> Band ^a (mag)
Peak mag.....	16.76 ± 0.03	≤16.65 ± 0.05	≤16.39 ± 0.21
Peak mag ^b	-19.02 ± 0.03	≤-19.13 ± 0.05	≤-19.39 ± 0.24
Host mag.....	18.99 ± 0.16	18.52 ± 0.22	18.69 ± 0.34
<i>A</i> _{galactic}	0.112 ± 0.003	0.071 ± 0.002	0.045 ± 0.001
<i>A</i> _{host} ^c	0.035 ± 0.003	0.022 ± 0.002	0.015 ± 0.001

^a Host-subtracted and extinction-corrected values.

^b $z = 0.0335$, $H_0 = 72 \text{ km s}^{-1}$, $\Omega_m = 0.3$, $\Omega_\Lambda = 0.7$.

^c $R_V = 3.1$.

a cubic spline for clarity. From the plot it can be seen that the shorter wavelength contribution to the bolometric flux of the SN emission is much higher near the onset of the event and steadily decreases after day 7 in the host frame (day ~ 9 in the observer frame). As a result, a broadening of the SED profile can also be seen at late times as the NIR contribution to the bolometric flux increases, consistent with the conclusions drawn from Figure 4. A much more detailed analysis and discussion of the evolution of the XRF 060218/SN 2006aj SED using our PAIRITEL observations in conjunction with optical *UBVr'i* photometry taken with the Mount Hopkins 48 inch telescope will be covered in Paper II (M. Modjaz et al. 2007, in preparation).

It is difficult to quantify the amount, if any, of the IR emission over the first 16 days that is a result of light echoes, a scenario in which the dust in the vicinity of the burst progenitor absorbs and then reradiates the optical and UV emission from the explosion. This would occur at a distance greater than the radius R_c at which the dust grains are destroyed due to sublimation, which when assuming a peak luminosity that is 70% of 1998bw gives a rough $R_c \sim 8\text{--}9 \text{ pc}$ (Waxman & Draine 2000). If the dust at this distance has a characteristic equilibrium temperature of $\sim 2300 \text{ K}$ (the temperature above which the grains are destroyed), then the resulting reradiated light would peak at $\nu \sim 2(1+z) \mu\text{m}$, where z is the redshift of the event, which at low z corresponds roughly to the *K* band (Reichart 2001). Although the prompt UV and optical emission along the line of sight could contribute IR emission on any timescale, the majority of the reradiated light is expected to be delayed as emission arrives from higher latitudes. We con-

clude that this effect, if present, contributes very little to our overall photometry primarily because the large sublimation radius would make the peak in the reradiated light occur beyond our last observation on day 16. Furthermore, a time-varying excess in the *K_s* would be expected if this effect were significant, which is not reflected in the SED. These values are summarized in Tables 2 and 3.

4. DISCUSSION

There is no significant evidence that any of the individual NIR *JHK_s* light curves observed with PAIRITEL peaks significantly faster than the others, although the *H* and *K_s* light curves are expected to peak after the *J* band, which would occur outside of our observation window. Furthermore, the rise profile in the individual *J*, *H*, and *K_s* bands before the peak appears to be largely independent of wavelength, with the light curve in each filter exhibiting roughly the same slope. This would make the chromatic rise-time properties of SN 2006aj consistent with bolometric rise-time results reported by Yoshii et al. (2003) for SN 2002ap and points to little or no spectral evolution in the NIR in the days preceding peak brightness. This can be seen in the color difference plot shown in Figure 5, which shows no significant trend in color evolution between the IR wavelengths during the rise portion of the burst. Furthermore, the sharp *V*-band peak reported by Modjaz et al. (2006), Sollerman et al. (2006), and Mirabal et al. (2006a) points to a relatively large increase in the NIR contribution to the total flux output after day ~ 10 .

The disagreements between the X-ray and optically inferred extinctions are striking but not uncommon in the literature (e.g., Campana et al. 2006; Guenther et al. 2006; Sollerman et al. 2005; Wiersema et al. 2007; Watson et al. 2007). As mentioned above, GRB host galaxies tend to have lower dust-to-metals ratios than, and probably extinction laws that deviate from, that of the Galaxy, possibly explaining the discrepancy between the N_{H} and N_{H} determined extinction values. Furthermore, Watson et al. (2007) have reported on a disagreement between the N_{H} column densities as inferred from $\text{Ly}\alpha$ absorption to the metal column densities from soft X-ray absorption, which they speculate is because the two diagnostics do not probe the same gas environments. Their results would imply that the N_{H} column measured from the early X-ray data would have the effect of overestimating the extinction that would be inferred through the use of the A_V - N_{H} relation, possibly explaining the disagreement described in § 3. Therefore, the exact host extinction could be the effect of a complex picture that is still not completely understood. Fortunately, this disagreement on the host galaxy extinction affects our NIR data far less than those at shorter wavelengths, highlighting the importance of NIR observations.

If we consider day 13 as being the onset of the NIR plateau phase of SN 2006aj, then the broad *J*-band peak would occur

TABLE 3
XRF 060218/SN 2006aj ABSOLUTE MAGNITUDES

Days Since GRB ^a	<i>J</i> Band ^{b,c} (mag)	<i>H</i> Band ^{b,c} (mag)	<i>K_s</i> Band ^{b,c} (mag)
1.92.....	-17.64 ± 0.09	-17.92 ± 0.21	-18.13 ± 0.49
2.88.....	-17.76 ± 0.09	-17.86 ± 0.33	-18.25 ± 0.15
3.88.....	-18.08 ± 0.19	-18.00 ± 0.17	-18.45 ± 0.10
4.81.....	-18.34 ± 0.03	-18.29 ± 0.13	-18.69 ± 0.22
5.79.....	-18.66 ± 0.06	-18.53 ± 0.14	-19.02 ± 0.48
6.73.....	-18.76 ± 0.08	-18.72 ± 0.13	-18.96 ± 0.11
7.71.....	-18.79 ± 0.05	-18.74 ± 0.33	-19.42 ± 0.14
8.67.....	-18.95 ± 0.07	-18.98 ± 0.12	-19.35 ± 0.19
9.65.....	-18.77 ± 0.07	-19.08 ± 0.04	...
12.56.....	-19.02 ± 0.05	-19.01 ± 0.03	-19.38 ± 0.24
13.54.....	-18.94 ± 0.02	-19.13 ± 0.05	...
14.47.....	-19.01 ± 0.03	-19.04 ± 0.06	-19.19 ± 0.11

^a Rest frame of GRB.

^b Host-subtracted and extinction-corrected values.

^c $z = 0.0335$, $H_0 = 72 \text{ km s}^{-1}$, $\Omega_m = 0.3$, $\Omega_\Lambda = 0.7$.

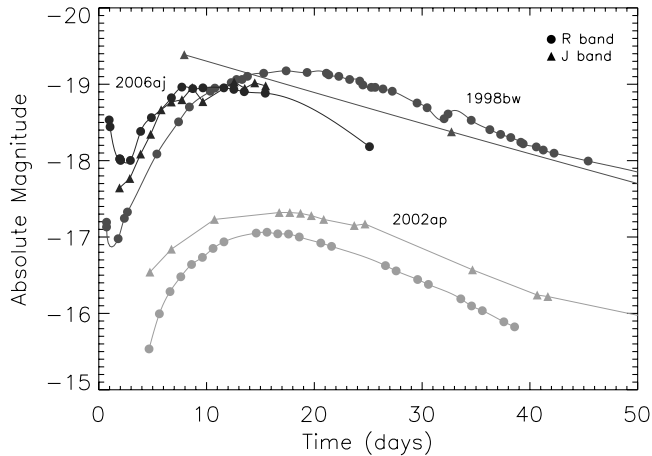


FIG. 6.—Comparison of the R - and J -band light-curve properties of XRF 060218/SN 2006aj (PAIRITEL), GRB 980425/SN 1998bw (Galama et al. 1998), and SN 2002ap (Foley et al. 2003; Yoshii et al. 2003). We use the explosion date of January 28.9 UT (JD = 2,452,303.4) inferred by Mazzali et al. (2002) as the $t = 0$ time for SN 2002ap. [See the electronic edition of the *Journal* for a color version of this figure.]

several days after the peak in the V band, which is estimated at 9.7 days in the rest frame by Modjaz et al. (2006). This would make our J -band rise time consistent with the previously observed trend in most SNe, in which the optical peak precedes the IR peak, as was the case with GRB 980425/SN 1998bw and SN 2003lw, both of which peaked 1.6 (Galama et al. 1998) and 5 (Malesani et al. 2004) days later in I band than in V band, respectively. The observed flattening of the NIR as early as day 10 makes SN 2006aj the fastest of the XRF/GRB-SNe observed to date, being substantially shorter in rise time than both GRB 980425/SN 1998bw and GRB 030329/SN 2003dh (Galama et al. 1998; Matheson et al. 2003). The fast evolution and plateau seen in SN 2006aj is reminiscent of the light-curve properties of broad-lined SNe Ic (SNe Ic BL), highly energetic core-collapse SNe, that do not show likely associations with GRBs. Two such events, SN 2002ap and SN 1997ef, have broad bolometric light curves, where the latter is estimated to peak in ~ 10 – 12 days, assuming the explosion date inferred by Mazzali et al. (2002). Similarly, our peak absolute magnitude of -19.02 ± 0.03 measured in J and -18.7 measured in V (Modjaz et al. 2006; Sollerman et al. 2006; Mirabal et al. 2006a) would make SN 2006aj the faintest of the XRF/GRB associated SNe, yet still brighter than the average broad-lined SN Ic. This can be seen in Figure 6, where the J - and R -band light curves of XRF 060218/SN 2006aj are plotted along the J - and R -band light curves of GRB 980425/SN 1998bw and SN 2002ap.

Both the peak luminosity and rise-time properties of SNe light curves are generally governed by the amount of ^{56}Ni produced in the explosion, leading many authors to conclude that the fast-evolving and underluminous nature of SN 2006aj points to smaller amounts of ^{56}Ni compared to other XRF/GRB-SNe. Modeling by Mazzali et al. (2006a) estimates the ^{56}Ni mass produced by SN 2006aj to be roughly $0.2 M_{\odot}$, compared to SN 1998bw and SN 2003dh, which are thought to have produced roughly 0.38 – 0.45 and 0.45 – $0.65 M_{\odot}$, respectively (Mazzali et al. 2006b). Yet, this low estimate of ^{56}Ni for SN 2006aj is still higher than the $\sim 0.09 M_{\odot}$ estimated for the SN 2002ap SN Ic BL (Foley et al. 2003), which reflects the amount typical produced by normal core-collapse SNe such as SN 1987A and SN 1994I.

SN 2006aj was also peculiar in several other aspects. First, the measured peak spectral energy of the gamma-ray emission $E_{\text{pk}} = 4.9$ keV, where E_{pk} is the maximum of the νF_{ν} spectra and hence where most of the gamma-ray energy is radiated, is extremely soft. This is in comparison to the GRB counterparts of SN 1998bw, 2003dh, and 2003lw, which all had E_{pk} values of roughly 55, 79, and 159 keV, respectively. Furthermore, the modeling done by Mazzali et al. (2006a) estimates an explosion kinetic energy of $E_K \approx 2 \times 10^{51}$ ergs and total ejected mass of $M_{\text{ej}} \approx 2 M_{\odot}$, both of which are lower than the values estimated for the other SNe with associated GRBs, but yet on the high end of the distribution of these values when compared to normal SN Ic events. Considering these relatively low E_{pk} , E_K , and M_{ej} values along with the low luminosity and fast rise time, it becomes clear that GRB 060218/SN 2006aj was indeed a peculiar type of event. It is quite likely that SN 2006aj, with its low E_K and M_{ej} values, is an intermediate type of event: extreme in many ways when compared to broad-lined core-collapse SNe like SN 2002ap and 1997ef that emit little or no high-energy emission, but rather weak when compared to previously observed XRF/GRB-SNe. Li (2006) has recently quantified a previously observed trend that correlates a GRB's E_{pk} value and the peak luminosity of its SNe emission, and hence the produced ^{56}Ni mass. Using this correlation, he estimates that the E_{pk} values for SN 2002ap and 1997ef, if they had possessed an associated GRB, would have occurred in the UV, far below the range of what is considered a GRB or XRF. This of course is based on the assuming this correlation is real and not an artifact of observational biases or source evolution. All of the SN 2006aj properties discussed above place it between the previously observed GRB-SNe sample and these low-luminosity and low-estimated E_{pk} broad-lined events, possibly pointing to a continuous distribution of SN events that emit at increasingly higher energies.

One possible explanation for such a continuous distribution of gamma-ray energies is that the soft-spectrum and low-luminosity events like XRF 060218 are due to off-axis observations of typical long-duration GRB-SNe (Yamazaki et al. 2003). Although this off-axis scenario was originally invoked to explain the peculiar high-energy properties of GRB-SNe like SN 1998bw, recent numerical simulations performed by Maeda et al. (2006) have shown that the viewing angle of asymmetric explosions would also have an effect on the observed luminosity and time of peak of the associated SNe. Through the use of three-dimensional Monte Carlo simulations, the authors find that asymmetric SNe would appear to peak earlier when viewed at small θ from the z -axis of the explosion, this being due primarily to low and extended ^{56}Ni densities in that direction. The resulting luminosity as seen in the z -direction is then boosted correspondingly because the photons can only diffuse out in this direction. This small θ scenario would then predict fast-peaking, high-luminosity, and high E_{pk} events, which is inconsistent with the parameter distribution seen in XRF 060218, which has a distinctly fast time to peak but a remarkably low luminosity and E_{pk} . Another difficulty of the off-axis interpretation is that it would require a very large intrinsic total energy of roughly $\sim 10^{53}$ ergs, which would be inconsistent with the relatively low kinetic energy measurements made from radio observations (Soderberg et al. 2006) at late times when the jet collimation and/or SNe asymmetry should no longer be significant. Furthermore, the probability of seeing a jet off-axis goes down significantly with increasing θ_j , resulting in inconsistent rate ratios between high- and low-energy events, as noted by Cobb et al. (2006). Therefore, although off-axis models can be made to successfully explain the observed range of GRB/XRF energetics, the range of SN properties such as E_K and M_{ej} , the measurements

of which are generally independent of collimation, suggest that viewing angle effects alone cannot account for the full diversity of XRF/GRB-SN properties.

On the other hand, the distribution of the intrinsic properties of the progenitor star that would lead to such a continuous distribution in the observed XRF/GRB-SN properties is also not entirely clear. A qualitative correlation between the estimated progenitor mass and the resulting explosive energy seen among several broad-lined and normal core-collapse SNe (Mazzali et al. 2002) points to a high initial stellar mass along with the progenitor's rotation rate, both of which would govern whether the jet associated with the GRB breaks out of the progenitor, as likely candidates. Nonetheless, future broadband observations of intermediate events like SN 2006aj and SN 2002ap may be crucial to the examination of this distribution.

Finally, we note that the Gorosabel et al. (2006) have reported evidence of a possible circularization of the explosion geometry, which like previous XRF/GRB-SNe is thought to be aspherical at early times (Mazzali et al. 2001; Hjorth et al. 2003). The authors show a rotation in the polarization angle of $\sim 90^\circ$ at 14 days $\lesssim t \lesssim 39$ days, which they interpreted as a circularization of the previous highly aspherical geometry. Similarly, Pian et al. (2006) reported a change in the decay slope of the photospheric expansion velocities versus time as determined through modeling of the spectra at the various epochs, which could also be interpreted as evidence for circularization. This circularization time of $t \sim 14$ roughly corresponds with the onset of the plateau phase in our NIR observations of SN 2006aj. One could

speculate that the fast rise observed in SN 2006aj is a result of fast and aspherical outflow that becomes spherical after $t \sim 14$ days, creating the observed plateau phase. However, the fact that a general broadening of SN light curves in the NIR is seen in other types of (presumably spherical) SN events would point to a mechanism common to all SNe, such as radiative transfer and/or the ionization changes in the SN ejecta (Kasen 2006), rather than the geometry of the explosion. Future NIR observations on the existence, or lack thereof, of a NIR plateau in normal (non-broadlined) SN Ic along with late-time spectral modeling and polarization measurements should shed light on any potential correlation between the explosion geometry and the resulting NIR light curve.

The Peters Automated Infrared Imaging Telescope (PAIRITEL) is operated by the Smithsonian Astrophysical Observatory (SAO) and was made possible by a grant from the Harvard University Milton Fund, the camera loan from the University of Virginia, and the continued support of the SAO and UC Berkeley. Partial support for PAIRITEL operations and this work comes from NASA grant NNG 06GH50G ("PAIRITEL: Infrared Follow-up for *Swift* Transients"). This work was conducted under the auspices of a DOE SciDAC grant (DE-FC02-06ER41453), which provides support to J. S. B.'s group. J. S. B. thanks the Sloan Research Fellowship for partial support. D. K. acknowledges financial support through the NSF Astronomy and Astrophysics Postdoctoral Fellowships under award AST 05-02502.

REFERENCES

- Alard, C. 2000, *A&AS*, 144, 363
 Barbier, L., et al. 2006, *GCN Circ.* 4780, <http://gcn.gsfc.nasa.gov/gcn/gcn3/4780.gcn3>
 Bertin, E., & Arnouts, S. 1996, *A&AS*, 117, 393
 Bloom, J., Starr, D., Blake, C., Skrutskie, M., & Falco, E. 2006, in *ASP Conf. Ser. 351, Astronomical Data Analysis Software and Systems XV*, ed. C. Gabriel et al. (San Francisco: ASP), 751
 Bloom, J., et al. 2004, *AJ*, 127, 252
 Butler, N. 2007, *ApJ*, 656, 1001
 Butler, N., et al. 2006, *ApJ*, 652, 1390
 Campana, S., et al. 2006, *Nature*, 442, 1008
 Cardelli, J., Clayton, G., & Mathis, J. 1989, *ApJ*, 345, 245
 Cobb, B. E., Bailyn, C. D., van Dokkum, P. G., & Natarajan, P. 2006, *ApJ*, 645, L113
 Cohen, M., Wheaton, W. A., & Megeath, S. T. 2003, *AJ*, 126, 1090
 Colgate, S. A. 1968, *Canadian J. Phys.*, 46, 476
 Cool, R., et al. 2006, *GCN Circ.* 4777, <http://gcn.gsfc.nasa.gov/gcn/gcn3/4777.gcn3>
 Cusumano, G., et al. 2006a, *GCN Circ.* 4775, <http://gcn.gsfc.nasa.gov/gcn/gcn3/4775.gcn3>
 ———. 2006b, *GCN Circ.* 4786, <http://gcn.gsfc.nasa.gov/gcn/gcn3/4786.gcn3>
 D'Avanzo, P., et al. 2006, *GCN Circ.* 4810, <http://gcn.gsfc.nasa.gov/gcn/gcn3/4810.gcn3>
 Dickey, J. M., & Lockman, F. J. 1990, *ARA&A*, 28, 215
 Foley, R. J., et al. 2003, *PASP*, 115, 1220
 Fruchter, A. S., & Hook, R. N. 1997, *Proc. SPIE*, 3164, 120
 Fruchter, A. S., et al. 2006, *Nature*, 441, 463
 Fukugita, M., et al. 1995, *PASP*, 107, 945
 Hicken, M., et al. 2006, *GCN Circ.* 4898, <http://gcn.gsfc.nasa.gov/gcn/gcn3/4898.gcn3>
 Hjorth, J., et al. 2003, *Nature*, 423, 847
 Galama, T., et al. 1998b, *Nature*, 395, 670
 Gorosabel, J., et al. 2006, *A&A*, 459, L33
 Guenther, E. W., Klose, S., Vreeswijk, P., Pian, E., & Greiner, J. 2006, *GCN Circ.* 4863, <http://gcn.gsfc.nasa.gov/gcn/gcn3/4863.gcn3>
 Jakobsson, P., et al. 2003, *A&A*, 408, 941
 Kasen, D. 2006, *ApJ*, 649, 939
 Kewley, L., et al. 2007, *AJ*, 133, 882
 Li, L.-X. 2006, *MNRAS*, 372, 1357
 Lipkin, Y., et al. 2004, *ApJ*, 606, 381
 Maeda, K., Mazzali, P., & Nomoto, K. 2006, *ApJ*, 645, 1331
 Malesani, D., et al. 2004, *ApJ*, 609, L5
 Masetti, N., Palazzi, E., Pian, E., & Patat, F. 2006, *GCN Circ.* 4803, <http://gcn.gsfc.nasa.gov/gcn/gcn3/4803.gcn3>
 Matheson, T., et al. 2003, *ApJ*, 599, 394
 Mazzali, P. A., Nomoto, K., Patat, F., & Maeda, K. 2001, *ApJ*, 559, 1047
 Mazzali, P. A., et al. 2002, *ApJ*, 572, L61
 ———. 2006a, *Nature*, 442, 1018
 ———. 2006b, *ApJ*, 645, 1323
 Mirabal, N., et al. 2006a, *GCN Circ.* 4792, <http://gcn.gsfc.nasa.gov/gcn/gcn3/4792.gcn3>
 ———. 2006b, *ApJ*, 643, L99
 Modjaz, M., et al. 2006, *ApJ*, 645, L21
 Pian, E., et al. 2006, *Nature*, 442, 1011
 Predehl, P., & Schmitt, J. H. M. M. 1995, *A&A*, 293, 889
 Reichart, D. 2001, *ApJ*, 554, 643
 Savaglio, S., & Fall, S. M. 2004, *ApJ*, 614, 293
 Schlegel, D., et al. 1998, *ApJ*, 500, 525
 Skrutskie, M., et al. 2006, *AJ*, 131, 1163
 Soderberg, A., et al. 2006, *Nature*, 442, 1014
 Sollerman, J., et al. 2005, *A&A*, 429, 559
 ———. 2006, *A&A*, 454, 503
 Stanek, R., et al. 2006, *Acta Astron.*, 56, 333
 Vreeswijk, P. M., et al. 2004, *A&A*, 419, 927
 Watson, D., et al. 2006, *ApJ*, 652, 1011
 ———. 2007, *ApJ*, 660, L101
 Waxman, E., & Draine, B. T. 2000, *ApJ*, 537, 796
 Wiersema, K., et al. 2007, *A&A*, 464, 529
 Woosley, S. 1993, *ApJ*, 405, 273
 Woosley, S., & Bloom, J. 2006, *ARA&A*, 44, 507
 Yamazaki, R., Daisuke, Y., & Nakamura, T. 2003, *ApJ*, 594, L79
 Yoshii, Y., et al. 2003, *ApJ*, 592, 467